

## RESEARCH ARTICLE

# The impact of wildfire on baseflow recession rates in California

Ryan R. Bart<sup>1</sup>  | Christina L. Tague<sup>2</sup>

<sup>1</sup>Department of Geography, San Diego State University, 5500 Campanile Drive, San Diego, CA 92182, USA

<sup>2</sup>Bren School of Environmental Science and Management, University of California, Santa Barbara, 2400 Bren Hall, Santa Barbara, CA 93106, USA

**Correspondence**

Ryan R. Bart, Earth Research Institute, University of California, Santa Barbara, 6832 Ellison Hall, Santa Barbara, CA 93106, USA.  
Email: ryanrbart@ucsb.edu

**Abstract**

The effect of wildfire on peak streamflow and annual water yield has been investigated empirically in numerous studies. The effect of wildfire on baseflow recession rates, in contrast, is not well documented. The objective of this paper was to quantify the effect of wildfire on baseflow recession rates in California for both individual watersheds and for all the study watersheds collectively. Two additional variables, antecedent groundwater storage and potential evapotranspiration, were also investigated for their effect on baseflow recession rates and postfire baseflow recession rate response. Differences between prefire and postfire baseflow recession rates were modeled statistically in 8 watersheds using a mixed statistical model that accounted for fixed and random effects. For the all-watershed model, antecedent groundwater storage, potential evapotranspiration, and wildfire were each found to be significant controls on baseflow recession rates. Wildfire decreased baseflow recession rates 52.5% (37.6% to 66.0%), implying that postfire reductions in above-ground vegetation (e.g., decreased interception, decreased evapotranspiration) were a stronger control on baseflow recession rate change than hydrophobicity. At an individual watershed scale, baseflow recession rate response to wildfire was found to be sensitive to intraannual differences in antecedent groundwater storage in 2 watersheds, with the effect of wildfire on baseflow recession rates being greater with lower levels of antecedent groundwater storage. Examination of burn severity for a subset of the study watersheds pointed to riparian zone burn severity as a potential primary control on postfire recession rate change. This study demonstrates that wildfire may have a substantial impact on fluxes to and from groundwater storages, altering the rate at which baseflow recedes.

**KEYWORDS**

baseflow, California, groundwater, mixed model, recession curve, wildfire

## 1 | INTRODUCTION

Wildfire alters landscapes by eliminating above-ground vegetation cover and increasing hydrophobicity in soils (Ice, Neary, & Adams, 2004). These modifications, in turn, may affect watershed hydrology by modifying vegetation interception, soil infiltration, and evapotranspiration (ET). In Mediterranean-climate regions (MCRs), which are located in parts of Australia, California, Chile, the Mediterranean Basin, and South Africa and distinguished by their climate regime of warm, dry summers and cool, wet winters, wildfires have been shown to increase peak flows that produce flooding and debris flows (Cannon, Gartner, Wilson, Bowers, & Laber, 2008; Keller, Valentine, & Gibbs, 1997; Wells, 1987) and increase annual flows that are important for local water supplies (Bart, 2016; McMichael & Hope, 2007). However, the effect of wildfire on baseflow, and in particular baseflow recession rates, is more uncertain. Baseflow recession rates are a key tool for low

flow prediction (Tague & Grant, 2009) and hydrologic modeling (Tallaksen, 1995) and provide insight into the mechanisms that control baseflow generation. Understanding the role of wildfire on baseflow recession rates is important in MCRs such as California that are subject to frequent wildfire and droughts, both of which are expected to increase in the future (Abatzoglou & Williams, 2016; Cook, Ault, & Smerdon, 2015).

The effect of wildfire on baseflow in MCRs has primarily been examined during the summer dry period when potential evapotranspiration (PET) is high and recharge to storage is negligible. Baseflow volumes during this period have been shown to increase following wildfire (Colman, 1951; Crouse, 1961; Kinoshita & Hogue, 2011, 2015), and postfire baseflow recession rates have been shown to decrease following the last storms of the wet season (Crouse, 1961; Meixner & Wohlgemuth, 2003). Less is understood about how wildfire affects baseflow during the wet season, when PET is lower and

recharge to storage is more dynamic. Jung, Hogue, Rademacher, and Meixner (2009) found that baseflow response to wildfire during the wet season was variable in two adjacent southern California watersheds, with postfire baseflow volume increasing in one watershed but not in the other. No known studies have examined the impact of wildfire on baseflow recession rates during the MCR wet season.

Baseflow recession rates in MCRs have been shown to vary intra-annually with changes in antecedent groundwater storage and PET. Lower baseflow recession rates have been associated with higher levels of antecedent groundwater storage in California watersheds (Bart & Hope, 2014). Meanwhile, higher baseflow recession rates have been associated with higher rates of PET for MCR watersheds in Australia and Turkey (Aksoy & Wittenberg, 2011; Wittenberg & Sivapalan, 1999). The effect of these intra-annual controls on baseflow recession rate response to wildfire is unclear.

The primary objective of this study was to quantify the effect of wildfire on baseflow recession rates in California for both individual watersheds and for all the study watersheds collectively. Although the effect of other forms of land-cover or land-use change on baseflow recession rates have been previously examined (Bogaart, van der Velde, Lyon, & Dekker, 2016; Federer, 1973), the effects of wildfire remain unresolved. Differences between prefire and postfire baseflow recession rates were modeled statistically in eight watersheds using a mixed statistical model that accounted for fixed and random effects (Hox, 2002; Raudenbush & Bryk, 2002). The secondary objective of this study was to investigate how antecedent groundwater storage and PET affect baseflow recession rate response to wildfire.

## 2 | THE EFFECT OF WILDFIRE ON GROUNDWATER FLUXES

Groundwater discharge to a stream  $Q_{GW}$  varies as a function of groundwater storage  $S_{GW}$ :

$$Q_{GW} = f(S_{GW}). \quad (1)$$

The rate at which  $Q_{GW}$  decreases over time depends on the size, geometry, porosity, saturated hydraulic conductivity, distribution, and connectivity of groundwater stores (Brutsaert & Nieber, 1977; Chen & Wang, 2013; Moore, 1997).  $S_{GW}$  is frequently affected by additional

fluxes besides  $Q_{GW}$  (Figure 1). These fluxes may include ET directly from groundwater  $ET_{GW}$  (Kirchner, 2009; Szilagyi, Gribovszki, & Kalicz, 2007) and recharge to groundwater  $R_{GW}$ , such that

$$\Delta S_{GW} = f(ET_{GW}, R_{GW}, Q_{GW}). \quad (2)$$

Fluxes operating concurrently (i.e., during the recession period) with  $Q_{GW}$  alter the rate of groundwater storage depletion and thus the baseflow recession rate.

Wildfire directly decreases  $ET_{GW}$  by reducing above-ground vegetation with access to the watertable and/or the capillary fringe (i.e., phreatophytes; Figure 1). Phreatophytes are located predominantly in and around riparian zones where the watertable is shallow (Tsang, Hornberger, Kaplan, Newbold, & Aufdenkampe, 2014) and changes in  $ET_{GW}$  are likely to be most sensitive to vegetation transformation within this zone (Le Maitre, Scott, & Colvin, 1999).  $ET_{GW}$  may vary seasonally, increasing when PET rates are highest. Changes in postfire  $ET_{GW}$  may persist for years depending on the length of postfire vegetation recovery (Hope, Albers, & Bart, 2012; Ireland & Petropoulos, 2015).

Wildfire also affects  $R_{GW}$  by altering water content above the  $S_{GW}$  water table (Figure 1).  $R_{GW}$  during the recession period may occur from upslope groundwater stores  $S_{GW-upslope}$ , where  $R_{GW}$  can be sustained following the end of a storm event (Jencso et al., 2009).  $R_{GW}$  from the unsaturated soil matrix  $S_{soil}$  is likely to be limited to the period immediately after a precipitation event and thus having little effect on baseflow recession rates. Elevated  $S_{soil}$  and  $S_{GW-upslope}$  levels may occur when postfire reductions in above-ground vegetation decrease transpiration from these stores (Silberstein, Dawes, Bastow, Byrne, & Smart, 2013). Elevated  $S_{soil}$  and  $S_{GW-upslope}$  levels may also occur when reduced levels of interception increase soil infiltration  $R_{soil}$  during storm events. Soil hydrophobicity, in contrast, may lower postfire  $S_{soil}$  and  $S_{GW-upslope}$  levels by decreasing  $R_{soil}$  during storm events (Letey, 2001). The relative size of  $S_{GW}$  and  $S_{GW-upslope}$  will depend on the watershed. In the topographically complex watersheds,  $S_{GW}$  may be limited to riparian zones, but upslope  $S_{GW-upslope}$  are likely to be highly variable (Jencso et al., 2009).

The overall effect of wildfire on baseflow recession rates depends on the net change in nondischarge postfire groundwater flux during the recession period. A net gain in  $S_{GW}$  during the recession

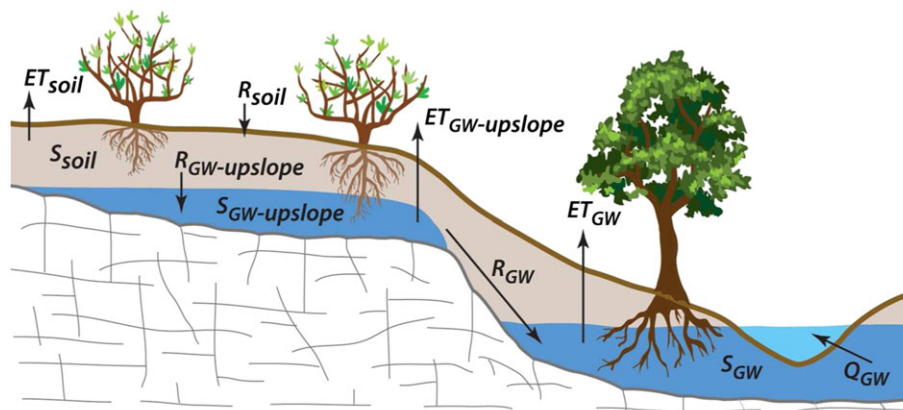


**FIGURE 1** Conceptual model of fluxes affecting baseflow recession rates. ET = evapotranspiration

period (i.e., slower groundwater depletion rate) decreases baseflow recession rates and implies that processes related to postfire reductions in above-ground vegetation (e.g., decreased interception, decreased ET) are the dominant hydrologic control. Alternatively, a net loss in  $S_{GW}$  during the recession period (i.e., faster groundwater depletion rate) increases baseflow recession rates and implies that processes related to hydrophobicity are the dominant hydrologic control.

### 3 | WATERSHEDS

Watersheds in this study were selected from all available US Geological Survey (USGS) streamflow network gauges in southern and central California. Watersheds were evaluated for inclusion based on absence of major diversions or regulations (e.g., dams), lack of persistent winter snow cover, limited (less than 5%) urbanization or agriculture, data quality, and having no additional large wildfires (greater than 5% of watershed area) during the prefire and postfire periods. Wildfire history for each watershed was obtained from the Fire and Resource Assessment Program (<http://frap.fire.ca.gov>). Daily streamflow data were acquired from the USGS ([waterdata.usgs.gov](http://waterdata.usgs.gov)). Daily precipitation totals were generated by merging two gridded precipitation data products: the monthly, 2.5 arcminute Precipitation-elevation Regressions on Independent Slopes Model produced at Oregon State University (<http://prism.oregonstate.edu>), and the daily, 15 arcminute US Unified Precipitation dataset provided by the National Oceanic and Atmospheric Administration Climate Prediction Center (<http://www.esrl.noaa.gov/psd>), in order to improve the temporal and spatial resolution over that of the individual data sets (Hope, Decker, & Jankowski, 2008). Daily gridded temperature data was obtained from the National Oceanic and Atmospheric

Administration Climate Prediction Center ([ftp://ftp.cpc.ncep.noaa.gov/precip/daily\\_grids](ftp://ftp.cpc.ncep.noaa.gov/precip/daily_grids)). Watershed characteristics were acquired from the Geospatial Attributes of Gages for Evaluating Streamflow database (Falcone, 2011).

Only eight watersheds were found suitable for analysis based on the selection criteria in this study. Watersheds with areas less than  $\sim 50$  km<sup>2</sup> had to be excluded due to the poor gauging precision of low flows for USGS gauges (Archfield & Vogel, 2009), which prevented an accurate representation of baseflow recession rates in those watersheds. Many additional watersheds had to be excluded due to the frequent occurrence of wildfires exceeding the 5% area threshold during the prefire and postfire analysis periods. A map and description of the eight selected watersheds is given in Figure 2 and Table 1, respectively. Daily streamflow data for the watersheds are available in S1. The watersheds are located along the Coast Range of central California and the Transverse Range of southern California. The watersheds are characterized by steep topography with peak elevations near 2000 m. The wet season extends from late fall (November) to early spring (April) and is dominated by cyclonic frontal systems approaching from the Pacific Ocean. Mean annual precipitation in the watersheds ranges from a little more than 600 mm to over 1100 mm. Mean annual streamflow is more variable, ranging from 120 mm to over 750 mm. During the summer dry season, flow ceases in many of the watersheds. The primary vegetation in most of the watersheds is chaparral shrubs, with grasslands, coastal sage scrub, oak woodlands, and forests also being common (Callaway & Davis, 1993).

Wildfire characteristics for each watershed are provided in Table 2. The percentage of area burned varied from 20% to 100% of the watershed area. The average length of the prefire period was 16.5 years, ranging from 11 to 19 years. A postfire length of 7 years was used for all watersheds except Nacimiento, which had only 3 years of postfire data available.

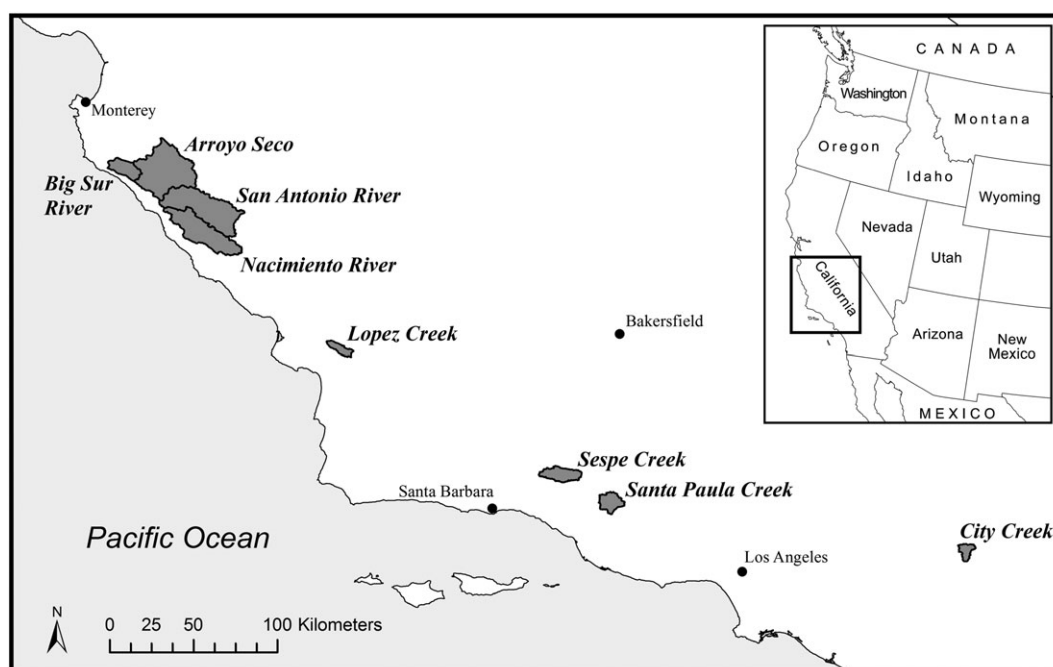


FIGURE 2 Location of study watersheds in California

**TABLE 1** Summary of watershed characteristics

Watershed name	USGS ID	Area (km <sup>2</sup> )	Mean annual precipitation (mm)	Mean annual PET (mm)	Mean annual streamflow (mm)	Dominant geology type	Mean slope (%)	Riparian zone forest percentage	Riparian zone shrub percentage
Arroyo Seco	11152000	625.1	809	664	243	sedimentary	34.7	48.4	40.6
Big Sur River	11143000	120.6	1,163	640	753	granitic	43.6	76.1	22.9
City Creek	11055801	50.5	781	729	226	quaternary	34.4	12.0	82.5
Lopez Creek	11141280	54.0	717	741	170	sedimentary	37.1	78.4	20.3
Nacimiento River	11148900	403.5	692	745	409	sedimentary	21.3	31.3	41.8
San Antonio River	11149900	556.4	633	737	174	sedimentary	19.5	21.8	36.2
Santa Paula Creek	11113500	103.3	678	709	220	sedimentary	34.4	34.9	53.0
Sespe Creek	11111500	128.5	850	552	120	sedimentary	26.5	41.2	50.4

Note. PET = potential evapotranspiration.

**TABLE 2** Fire characteristics, analysis periods, and calibration variables

Catchment	Fire year	Fire size (%)	Prefire period	Postfire period	Prefire events	Postfire events	Median <i>b</i> value	$\Delta Q_{crit}$ (mm)
Arroyo Seco	1977	63	1967–1977	1978–1984	42	45	2.058	0.1
Big Sur	1977	92	1967–1977	1978–1984	41	38	1.985	0.25
City	2003	94	1986–2003	2004–2010	27	11	1.872	0.4
Lopez	1985	100	1968–1985	1986–1992	26	4	1.716	0.4
Nacimiento	1996	20	1980–1996	1997–1999	95	17	1.954	0.1
San Antonio	1985	31	1967–1985	1986–1992	73	17	1.658	0.12
Santa Paula	1985	71	1967–1985	1986–1992	41	10	1.782	0.2
Sespe	1985	40	1967–1985	1986–1992	30	8	1.884	0.2

## 4 | METHODOLOGY

### 4.1 | Baseflow recession rates

Baseflow recession curves were defined as a consecutive decline in the streamflow hydrograph for 5 or more days following the exclusion of the first 2 days after a hydrograph stormflow peak to minimize the impact of storm-related flows. A daily precipitation threshold of 5 mm during the recession period was also included to account for precipitation events that may have decreased baseflow recession rates but not increased baseflow volumes.

Although baseflow recession curves may be analyzed directly from the recession limb of a streamflow hydrograph using an exponential or nonlinear model (Chapman, 1999; Wittenberg, 1999), Brutsaert and Nieber (1977) proposed comparing the rate of baseflow change  $dQ/dt$  to baseflow magnitude  $Q$  on a  $\log(-dQ/dt) - \log(Q)$  plot. This relation is represented as

$$-\frac{dQ}{dt} = f(Q). \quad (3)$$

The time variable is eliminated using this approach, allowing baseflow recession rates for a given baseflow magnitude to be comparable between baseflow recession curves. This relation is referred to as the recession slope curve (Rupp & Selker, 2006a) and frequently follows a power-law function

$$-\frac{dQ}{dt} = aQ^b, \quad (4)$$

where  $Q$  is baseflow discharge in mm,  $t$  is time (daily),  $a$  is the value of  $-dQ/dt$  when  $Q = 1$ , and  $b$  is the slope of the  $\log(-dQ/dt) - \log(Q)$

relation (Clark et al., 2009).  $dQ/dt$  was computed as the difference between two consecutive points on a baseflow recession curve,

$$\frac{dQ}{dt} = \frac{Q_i - Q_{i-1}}{\Delta t}, \quad (5a)$$

and  $Q$  was computed as the mean of two consecutive recession points,

$$Q = \frac{Q_i + Q_{i-1}}{2}. \quad (5b)$$

Low precision in the gauging of low flows may hinder investigations of the recession slope curve due to scatter and discretization associated with low magnitude recession flows on a  $\log(-dQ/dt) - \log(Q)$  plot. These errors were accounted for by increasing the time interval  $\Delta t$  for flows below the precision of the gauge until the change in baseflow  $\Delta Q$  over the time period exceeded a critical threshold  $\Delta Q_{crit}$  (Rupp & Selker, 2006b). The critical threshold was determined visually for each watershed (Table 2).

Previous studies have demonstrated that values of  $b$  in the power-law relation of Equation 4 are less variable than values of  $a$  (Biswal & Marani, 2010; Shaw, McHardy, & Riha, 2013). In this study, the exponent  $b$  was fixed at a common value for each watershed, leaving a single free parameter  $a$  for representing baseflow recession rates. The fixed value of  $b$  was derived by fitting a linear regression model with log-transformed data (Xiao, White, Hooten, & Durham, 2011) to each individual recession slope curve in a watershed and selecting the median  $b$  value from among all the curves (Table 2).  $a$  was then recomputed for all values along the recession slope curve using Equation 4 with the fixed  $b$ . The

median value of  $a$  from each individual recession slope curve was used to represent the baseflow recession rate for that recession slope curve. Baseflow recession data are available in S2.

### 4.2 | Mixed model

Baseflow recession curve data contains a hierarchical structure that does not conform to the independence assumption that is required for linear regression models (Watson, Vertessy, McMahon, Rhodes, & Watson, 2001). For individual watersheds, baseflow recession rates for individual recession events within a given year are likely to be more similar than between years. Baseflow recession rates represent the lower level of the hierarchy (i.e., level 1) and are nested within years, which represent the higher level of the hierarchy (i.e., level 2; Figure 3). When analyzing all watersheds collectively, the hierarchical structure becomes more complex, with baseflow recession rates nested within years that are nested within watersheds (Figure 3). This hierarchical structure is referred to as having three levels. Baseflow recession rates for analyzing all watersheds collectively may alternatively be nested by precipitation event (Figure 3). Watersheds with baseflow recession rates produced from the same precipitation event will likely be more similar than baseflow recession rates produced from different precipitation events due to similarities in antecedent groundwater storage across a region. Data with two hierarchical structures is referred to as having crossed random effects (Baayen, Davidson, & Bates, 2008).

Mixed modeling is a technique used to examine data containing a hierarchical structure (Hox, 2002). Mixed models account for hierarchies within data by partitioning model error to each level of the hierarchy using variables containing random effects. Random effects represent the stochastic portion of the model, and fixed effects represent the deterministic portion (Hox, 2002). A mixed model for representing the individual watershed-scale hierarchy in Figure 3 may be described as

$$y_{ij} = \beta_0 + \sum_{n=1}^N \beta_n x_{nij} + u_j + e_{ij}, \tag{6}$$

where  $y_{ij}$  is the  $i$ th observation of baseflow recession rates ( $a$ ) for the  $j$ th year,  $\beta_0$  is the intercept of the model,  $N$  is the total number of

predictor variables,  $\beta_n$  is the slope of the relation between the  $n$ th predictor variable and baseflow recession rates,  $x_{nij}$  is the  $i$ th observation of the  $n$ th predictor variable for the  $j$ th year,  $u_j$  is the level 2 model error for the  $j$ th year and  $e_{ij}$  is the level 1 model error for the  $i$ th observation from the  $j$ th year.

Model errors in mixed models are generally assumed to be independent and normally distributed with a mean of 0 and a variance of  $\sigma^2$ . However, autocorrelation of level 1 model errors may occur with longitudinal data such as baseflow recession rates if memory from one baseflow recession event affects subsequent events. In some cases, this autocorrelation may be explicitly modeled through the error covariance matrix (Hox, 2002). However, when the available data at the lowest hierarchical level is small, quantifying the autocorrelation can be challenging. Fortunately, the effect of autocorrelation on mixed modeling results, and particularly the fixed effects, has been shown to be negligible when level 1 sample sizes are small (Hox, 2002; Raudenbush & Bryk, 2002). The median number of baseflow recession events within a given year for this study was 3, ranging from 1 to 11. Because the primary objective was to understand how a fixed effect variable, wildfire, affects baseflow recession rates, level 1 autocorrelation was not explicitly accounted for in this study.

A mixed model for representing the all-watershed hierarchy in Figure 3 may be represented by

$$y_{i(jk \cdot l)} = \beta_0 + \sum_{n=1}^N \beta_n x_{ni(jk \cdot l)} + w_l + v_k + u_{jk} + e_{i(jk \cdot l)}, \tag{7}$$

where  $y_{i(jk \cdot l)}$  is the  $i$ th observation of baseflow recession rate from the cross-classified  $j$ th year and  $k$ th watershed with the  $l$ th precipitation event,  $x_{ni(jk \cdot l)}$  is the  $i$ th observation for the  $n$ th predictor variable from the cross-classified  $j$ th year and  $k$ th watershed with the  $l$ th precipitation event,  $w_l$  is the level 2 model error for the  $l$ th precipitation event,  $v_k$  is the level 3 model error for the  $k$ th watershed,  $u_{jk}$  is the level 2 model error for  $j$ th year in the  $k$ th watershed, and  $e_{i(jk \cdot l)}$  is the level 1 model error for the  $i$ th observation of baseflow recession rate from the cross-classified  $j$ th year and  $k$ th watershed with the  $l$ th precipitation event (Hox, 2002).

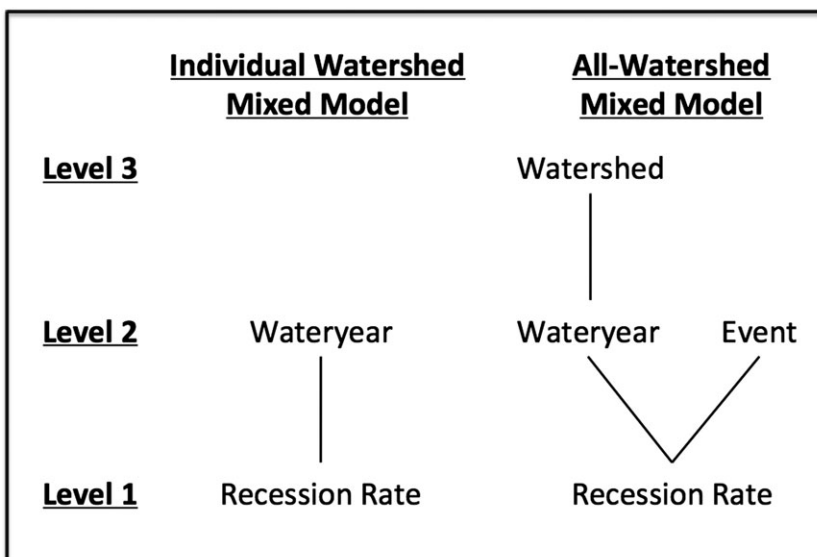


**FIGURE 3** Hierarchical structure for the individual watershed and the all-watershed mixed models

A Bayesian estimation procedure using Markov Chain Monte Carlo (MCMC) techniques was used to calibrate the mixed model (Stegmueller, 2013). A Gibbs sampling algorithm with an improper, noninformative prior was applied to each MCMC walk (Hadfield, 2010) and a Gaussian distribution was assumed for the likelihood. Each model was calibrated using 1,000,000 iterations with a thinning of 100. Model convergence was evaluated visually, and model performance was evaluated using the deviance information criterion (Hadfield, 2010),

$$DIC = \bar{D} + p_D. \quad (8)$$

$\bar{D}$  is a measure of model fit and defined as the mean deviance  $D$  from all MCMC iterations. Deviance is calculated as

$$D = -2 \ln(p(y|\theta)), \quad (9)$$

where  $p(y|\theta)$  is the likelihood function and  $\theta$  is a model parameter.  $p_D$  is a measure of model complexity, representing the effective number of model parameters (Spiegelhalter, Best, Carlin, & van der Linde, 2002). Smaller values of deviance information criterion signify better model fit. All mixed modeling was implemented using the MCMCglmm package (Hadfield, 2010) in the R programming language ([www.r-project.org](http://www.r-project.org)).

### 4.3 | Model parameters and development

In order to examine the effect of wildfire on baseflow recession rates, individual watershed (Equation 6) and all-watershed (Equation 7) mixed models were developed to predict  $a$  ( $\log_e$ ) from three watershed variables, antecedent groundwater storage ( $\log_e$ ), PET, and wildfire. These variables were selected a priori based on the hydrological processes that were expected to be important controls on baseflow recession rates, with antecedent groundwater storage and PET being key controls on intra-annual baseflow recession rates and wildfire being the primary variable of interest.

The seasonality of rainfall in California produces two hydrologic regimes: a water-limited summer dry season and an energy-limited winter wet season. Baseflow recession rates in central California watersheds have been shown to decrease as watershed storages are filled during the transition from the dry season to the wet season (Bart & Hope, 2014). To account for intra-annual differences in antecedent groundwater storage for this study, an estimate of antecedent groundwater storage for each baseflow recession event was developed using precipitation cumulated from the beginning of the water year (October 1) to the start of each baseflow recession curve. This proxy for antecedent groundwater storage is similar to that used in Bart and Hope (2014) but with precipitation substituted for streamflow because streamflow is a component of the dependent variable in the mixed model. Although cumulative antecedent precipitation cannot account for decreases in watershed storage between precipitation events, it was assumed that cumulative antecedent precipitation would provide a first-order approximation of antecedent groundwater storage for each recession event, as was the case with cumulative antecedent streamflow in Bart and Hope (2014).

PET for each recession curve was averaged from daily PET values over the recession period. Daily PET was derived from daily temperature data using the Blaney-Criddle transformation:

$$PET = p(0.457 * T + 8.13), \quad (10)$$

where  $PET$  is the estimated PET (mm/day),  $T$  is the mean daily temperature ( $^{\circ}\text{C}$ ), and  $p$  is the mean daily percentage of total annual daytime hours at  $35^{\circ}$  latitude (Blaney & Criddle, 1962).

The effect of wildfire on baseflow recession rates was incorporated into the model via a wildfire variable representing watershed conditions before and after wildfire. The variable ranged from 0 to 1, with 0 representing prefire (mature) vegetation conditions and 1 representing complete elimination of vegetation over 100% of the watershed. For the first postfire year, the change in watershed conditions was assumed to be equivalent to the percentage of watershed area burnt. For subsequent postfire years, the level of change in watershed conditions was equal to percent area burnt multiplied by a normalized postfire vegetation recovery curve (Bart, 2016) that was developed from remote sensing studies of chaparral recovery in central California (Hope, Tague, & Clark, 2007; McMichael, Hope, Roberts, & Anaya, 2004). The normalized post-fire vegetation recovery curve was computed as {1.00, 0.63, 0.50, 0.40, 0.32, 0.25, 0.19} for the first 7 years following wildfire. This wildfire variable was found to be the best predictor of postfire annual streamflow in California watersheds amongst several wildfire variables tested in Bart (2016).

Two interaction variables were separately incorporated into the mixed model in order to examine how antecedent groundwater storage and PET modify baseflow recession rate response to wildfire. The first interaction variable between wildfire and antecedent groundwater storage was generated from the product of the wildfire variable with the cumulative antecedent precipitation variable and investigated whether postfire baseflow recession rate change was sensitive to high or low wetness conditions. The second interaction variable between wildfire and PET was generated from the product of the wildfire variable with the PET variable and examined whether differences in PET rates produced different levels of postfire baseflow recession rate change.

For mixed models, predictor variables are often centered to contain a zero point in order to aid in the interpretation of model results (Aguinis, Gottfredson, & Culpepper, 2013). Following the recommendation of Enders and Tofighi (2007), for models directly investigating the effect of wildfire on baseflow recession rates (i.e., primary objective), cumulative antecedent precipitation and PET were grand-mean centered for the individual watershed models and group-mean centered by watershed for the all-watershed models. For all models investigating how interaction variables may modify the effect of wildfire on baseflow recession rates, cumulative antecedent precipitation and PET were group-mean centered by water year.

## 5 | RESULTS

The relation between baseflow recession rates ( $a$ ) and cumulative antecedent precipitation for each of the eight watersheds is displayed in Figure 4. Baseflow recession rates were separated by prefire and postfire with symbol size corresponding to PET rates during the recession event. Baseflow recession rates showed a decrease with higher cumulative antecedent precipitation and the relation between the two variables generally followed a power-law

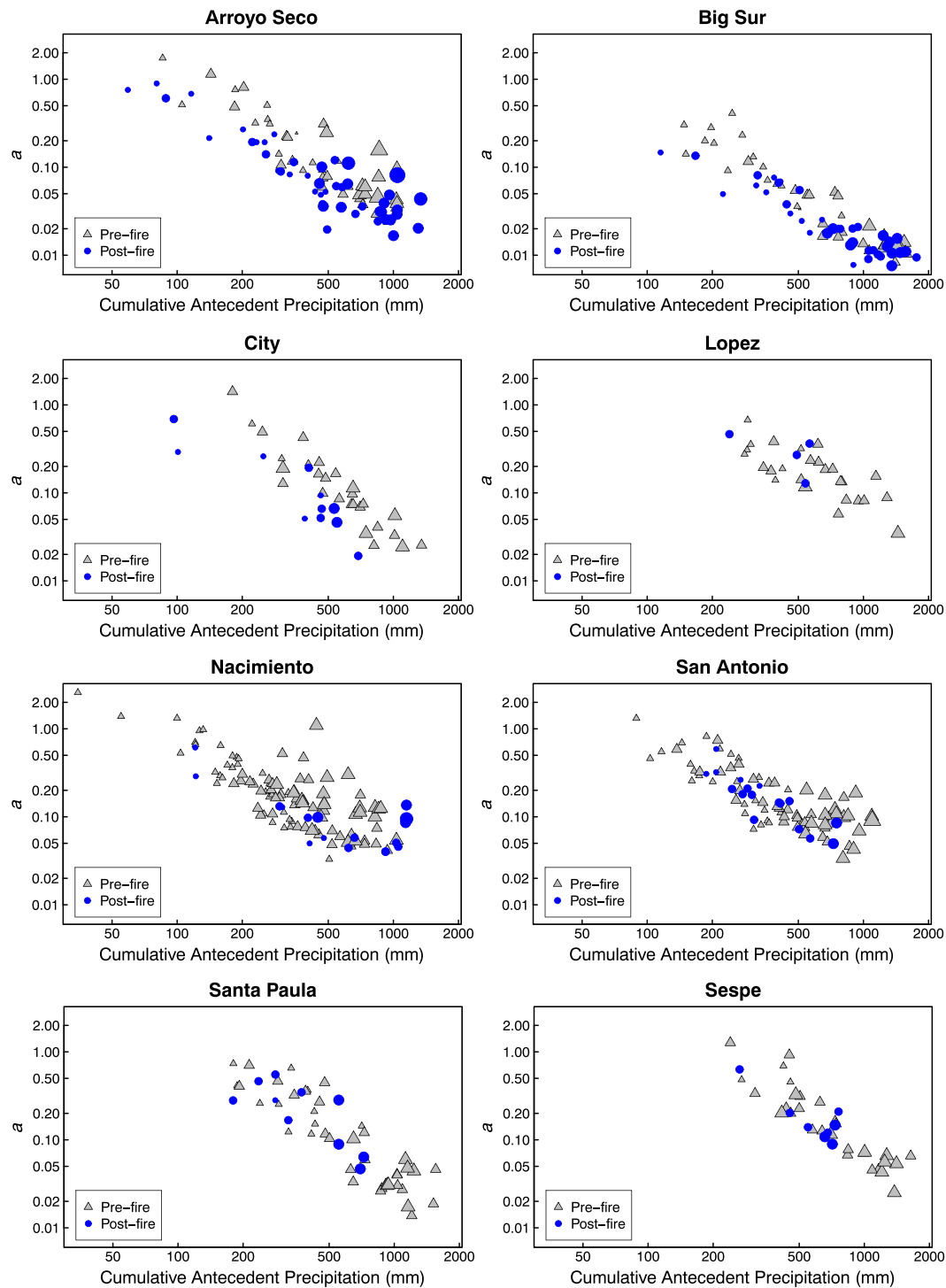


**FIGURE 4** Plots of  $a$  from Equation 4 against cumulative antecedent precipitation, separated by prefire and postfire baseflow. Larger symbols correspond to higher potential evapotranspiration (range 1.7 to 6.1 mm/day)

function. PET was slightly correlated with cumulative antecedent precipitation (Pearson's  $r = 0.61$  across all watersheds) because maximum PET values occur in the spring at the end of the wet season. The effect of correlation between these two independent variables on the mixed model is unclear. For a given level of cumulative antecedent precipitation, higher PET generally corresponded to a higher value of  $a$ , although this effect was not ubiquitous, such as in City or Sespe. Visually, postfire baseflow recession rates decreased relative to prefire baseflow recession rates in three watersheds, Arroyo

Seco, Big Sur, and City. Postfire baseflow recession rates in the five other watersheds did not exceed the variability of the prefire baseflow recession rates.

The values representing the mode and 95% credible (i.e., confidence) intervals for each of the four fixed parameters in the individual watershed and all-watershed models are presented in Figure 5. Two of the parameters, the intercept and cumulative antecedent precipitation, were highly significant (i.e., credible intervals do not cross 0) for all of the models. This supports the visual evidence in Figure 4 that baseflow

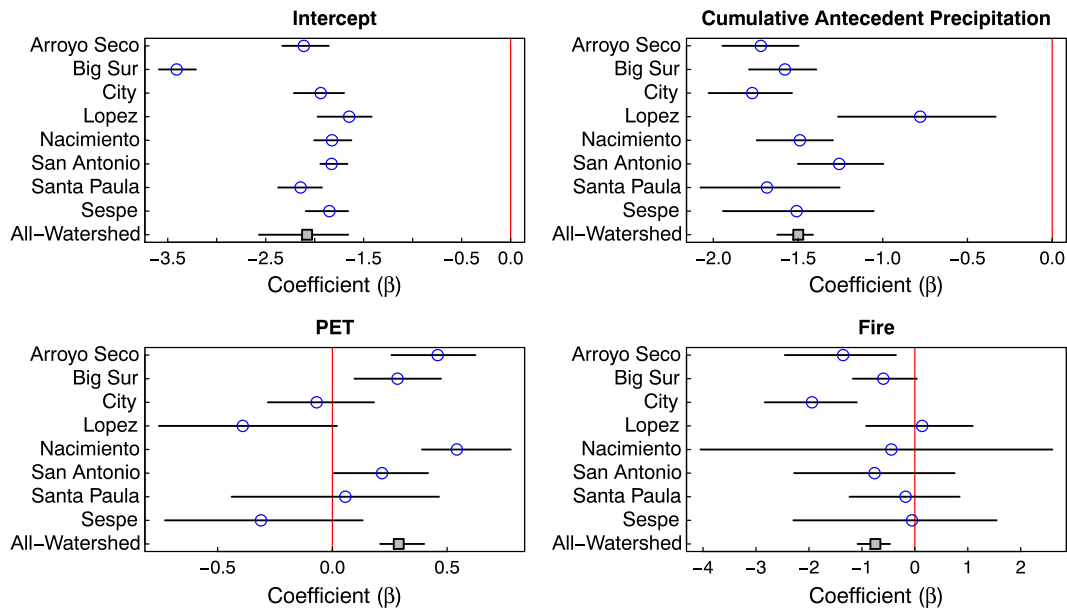


**FIGURE 5** Coefficient ( $\beta$ ) values and 95% credible intervals for intercept, cumulative antecedent precipitation, potential evapotranspiration (PET), and fire variables in the individual watershed and the all-watershed mixed models

recession rates decrease with higher levels of antecedent groundwater storage. For every doubling of cumulative antecedent precipitation, the value of  $a$  decreased by 64.6% (62.4% to 67.5%) for the all-watershed model.

The effect of PET on baseflow recession rates was more variable than cumulative antecedent precipitation, with four watersheds (Arroyo Seco, Big Sur, Nacimiento, San Antonio) showing significant increases in baseflow recession rates with higher rates of PET (Figure 5). These four watersheds were clustered in the Santa Lucia Mountains in the northern portion of the study region. The four northern watersheds also corresponded to the four watersheds with the most available data, averaging 92 baseflow recession events per watershed over the period-of-record versus 39 for the southern watersheds (Table 2). Thus, the effect of PET on baseflow recession rates for the all-watershed model was found to be statistically significant. The all-watershed model predicted that for every millimeter increase in daily PET the value of  $a$  would increase by 33.5% (23.2% to 49.1%).

At the individual watershed scale, baseflow recession rates showed a significant decrease following wildfire in two watersheds, Arroyo Seco and City (Figure 5), with a third watershed, Big Sur, being nearly significant. Four additional watersheds showed nonsignificant

decreases in baseflow recession rates, including Nacimiento, which had exceptionally wide uncertainty intervals due to having only 3 postfire years available for inclusion in the model (Table 2). Collectively, these results produced a significant decrease in postfire baseflow recession rate, with the all-watershed model predicting that  $a$  would decrease 52.5% (37.6% to 66.0%) during the first postfire year assuming 100% burnt. This effect decreases linearly with lower percentages of area burnt and nonlinearly according to the normalized postfire vegetation recovery curve following the first year.

The effect of intra-annual differences in cumulative antecedent precipitation on postfire baseflow recession rate change is shown in Figure 6. For two watersheds, Arroyo Seco and Big Sur, the interaction variable showed significant increases, indicating that greater change in postfire baseflow recession rates was observed with lower cumulative antecedent precipitation than with higher cumulative antecedent precipitation. None of the remaining individual watershed models, or the all-watershed model, showed significant changes in postfire baseflow recession rate response with cumulative antecedent precipitation. No value was obtained for Lopez due to limited postfire data.

The effect of PET on postfire baseflow recession rate change was small and insignificant for both the individual watershed and the all-watershed models (Figure 6).

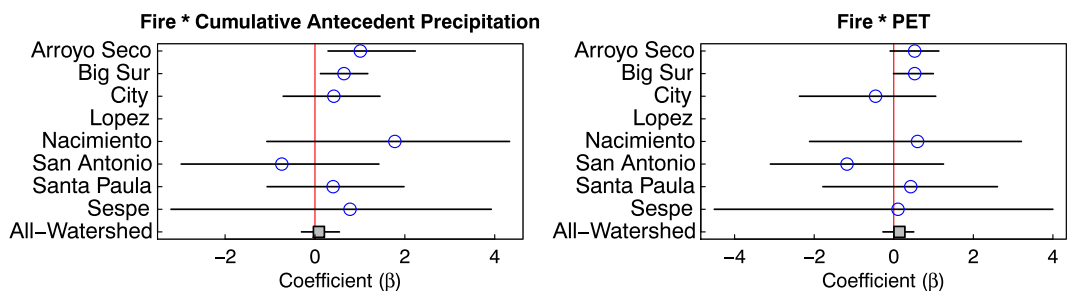


**FIGURE 6** Coefficient ( $\beta$ ) values and 95% credible intervals for interaction variables in the individual watershed and the all-watershed mixed models. PET = potential evapotranspiration

## 6 | DISCUSSION

The results from the mixed model analysis demonstrated that antecedent groundwater storage was the first-order control on baseflow recession rates in California watersheds, with lower baseflow recession rates associated with higher levels of antecedent storage (Figure 5). This result is consistent with recent studies in California watersheds that have suggested that decreases in baseflow recession rates may be related to either a shift in the dominant storages contributing to baseflow from small, quickly depleting stores to larger, slower depleting stores as the wet season progresses (Bart & Hope, 2014), or similarly, an expansion and contraction of the active drainage network (Biswal & Kumar, 2014). Across the watersheds, the effect of antecedent storage on baseflow recession rates was very similar (Figure 5), indicating that at individual watershed scales, the underlying mechanisms that cause baseflow recession rates to evolve as storages fill during the wet season are similar across the region.

A positive relation between PET and baseflow recession rates was observed with the all-watershed model and in the four northernmost individual watersheds of the study. No significant relation was observed in the four southern watersheds, which is similar to Tschinkel (1963) who found that the effect of ET on baseflow recession rates was negligible in a small watershed located near City Creek (Zecharias & Brutsaert, 1988). The sensitivity of baseflow recession rates to PET in the northern watersheds suggests that phreatophytes in the northern watersheds may have greater contact with groundwater than in the southern watersheds. However, the result is more likely due to an insufficient range of PET values in the southern watersheds to accurately characterize the relation between PET and baseflow recession rates. During the late spring (after May 1) when PET rates are highest, the southern watersheds averaged less than 2 recessions over the period of record versus 8.5 recessions for northern watersheds. The lack of large PET values associated with baseflow recession rates in the southern watersheds may have resulted in an ill-defined relation between PET and baseflow recession rates.

Following wildfire, baseflow recession rates in the all-watershed model decreased, which implies that there was a net gain to groundwater during the recession period, likely through a combination of decreased ET and/or decreased interception. It also implies that the long-term effect of soil hydrophobicity on baseflow recession rates was smaller than the effect of vegetation change, though the absolute effect of both is not known. At large scales, spatial heterogeneity in postfire hydrophobicity can diminish its capacity to

decrease soil infiltration and groundwater recharge (DeBano, 2000; Imeson, Verstraten, van Mulligen, & Sevink, 1992). Further, in some cases the temporal effects of hydrophobicity may be limited to the first few months following wildfire, depending on levels of hydrophobicity in the watershed and postfire meteorological conditions (Shakesby & Doerr, 2006). Consequently, it appears that baseflow recession rate change is primarily driven by postfire changes in ET and not hydrophobicity.

For individual watersheds, the effect of wildfire on baseflow recession rates was variable, with two watersheds showing large, significant decreases in baseflow recession rates, five watersheds showing small, nonsignificant decreases and one watershed showing a small, nonsignificant increase. For the watersheds in this study that were not significantly affected by wildfire, a lack of postfire change in baseflow recession rates may reflect limited postfire change in ET from groundwater ( $ET_{GW}$ ). This may occur when wildfire is either not located in areas of the watershed where vegetation is in contact with groundwater, such as the riparian zone, or when burn severity in these areas is low. In the current study, burn severity was not explicitly included in the mixed model because burn severity estimates via Monitoring Trends in Burn Severity (MTBS) products (Eidenshink et al., 2007) are not available for wildfires in two of the watersheds, Arroyo Seco and Big Sur. In order to get an indication of whether riparian zone burn severity may have been an important control on baseflow recession rate change, we qualitatively assessed the location and burn severity of wildfires in the six watersheds with available MTBS data using Google Earth (Table 3). MTBS classifies burn severity into five classes (unburned, low, moderate, high and increased greenness) based on the differenced Normalized Burn Ratio from Landsat images taken before and after a wildfire (Eidenshink et al., 2007).

The results of this post hoc analysis are consistent with riparian zone burn severity being an important control on postfire baseflow recession rate change. Of the six watersheds where burn severity data was available, the one watershed where postfire baseflow recession rate change was observed, City, was also the only watershed to show moderate to high levels of riparian zone burn severity (Table 3). The five remaining watersheds either had no burning in the riparian zone or the fire passed through the riparian zone but left the vegetation unburnt or burnt with low severity. While these results suggest that postfire riparian  $ET_{GW}$  may be a primary control on baseflow recession rate change, further analysis and additional data will be needed to substantiate this effect. A significant effect would mean that the frequency of postfire baseflow recession rate change may be related

**TABLE 3** Evaluation of riparian zone burn severity

Watershed	Postfire recession rate change observed?	Amount of riparian zone within burn perimeter	Severity of burnt riparian zone
Arroyo Seco	Yes	moderate	not available
Big Sur	No	large	not available
City	Yes	large	moderate to high
Lopez	No	large	unburned to low
Nacimiento	No	none	not applicable
San Antonio	No	none	not applicable
Santa Paula	No	large	unburned to low
Sespe	No	small	low to moderate

to riparian zone fire return intervals, which may differ from adjacent upland areas (Luce et al., 2012). In City, the percentage of riparian shrubs (82.5%) was much higher than in the other watersheds, however, it is unclear if this contributed to its higher riparian zone burn severity. Overall, riparian zone fire severity appears to be a potentially important variable for predicting postfire baseflow recession rate change.

Higher antecedent groundwater storage was found to reduce the effect of wildfire on baseflow recession rates in two watersheds, Arroyo Seco and Big Sur (Figure 6). Both of these watersheds were sensitive to PET, indicating that ET from groundwater was likely an important control on baseflow recession rates. During the early part of the wet season, baseflow in MCR watersheds has been hypothesized to be generated from small, quickly recharged groundwater stores that are likely to coincide with saturated riparian areas (Bart & Hope, 2014). As the wet season progresses, larger nonriparian groundwater stores ( $S_{\text{GW-upslope}}$ ) are filled and the primary control on baseflow recession rates shifts to these larger stores. For a given ET flux from groundwater, the effect on storage depletion will be proportionally larger for a smaller store than a larger store. Further, vegetation may have better access to shallow riparian stores than larger hillslope storages. Consequently, the effect of wildfire on baseflow recession rates could be expected to be greatest early in the wet season when phreatophyte vegetation have the greatest relative impact on groundwater stores contributing to baseflow. It would also be greatest during dry years, when decreases in baseflow recession rates may be most valuable to watershed managers. This effect, however, was not universal amongst the watersheds (Figure 6), possibly due to an insufficient amount of available postfire data to support the more complex interaction-variable model. As a result, weak statistical power for the all-watershed mixed model may have contributed to its nonsignificance.

PET did not show any effect on postfire baseflow recession rate change in this study (Figure 6). Many of the coefficient values indicated a decrease in baseflow recession rate response to wildfire with increasing potential ET, however, this is the opposite effect of what would be expected based on the physical processes operating in a watershed. These results suggest that the available data in this study may not support the complexity of the mixed model when an interaction term is included.

For the all-watershed model, baseflow recession rates were shown to decrease following wildfire. However, inference at this regional scale was limited, particularly in regard to interaction variables, due to the inclusion of only eight watersheds. A greater number of watersheds would allow for a more robust analysis of not only the level 1 interaction variables included in this study (i.e., cumulative antecedent precipitation and PET) but also level 2 interaction variables (e.g., watershed area and soil depth) that would allow an examination of how watershed characteristics affect baseflow recession rate change. The inclusion of more watersheds in California, however, will necessitate either relaxing the watershed selection criteria used in this study and/or waiting for more wildfires to occur in gauged watersheds.

In conclusion, the purpose of this paper was to examine the impact of wildfire on baseflow recession rates. The first-order control on baseflow recession rates was found to be intra-annual differences in

antecedent groundwater storage, with baseflow recession rates decreasing with increasing cumulative antecedent precipitation. Baseflow recession rates also increased with higher rates of PET, although this effect was highly variable amongst individual watersheds. The all-watershed model indicated that wildfire decreased baseflow recession rates 52.5% (37.6% to 66.0%) during the first postfire year assuming 100% burnt. This decrease implies that processes associated with postfire reductions in above-ground vegetation (e.g., decreased interception and decreased ET) were a stronger control on baseflow recession rates than hydrophobicity. At an individual watershed scale, baseflow recession rate response to wildfire was found to be sensitive to intra-annual differences in antecedent groundwater storage in two watersheds, with effect of wildfire on baseflow recession rates being greater with lower levels of antecedent groundwater storage. Examination of burn severity for a subset of the study watersheds pointed to riparian zone burn severity as a potential primary control on postfire recession rate change. This study demonstrates that wildfire can have a substantial impact on fluxes to and from groundwater storages, altering the rate at which baseflow recedes.

## ACKNOWLEDGMENTS

We thank Allen Hope for extensive discussion and comments on this paper. We also thank Trent Biggs and Oliver Chadwick for providing feedback, Janet Choate for graphical assistance, and the two manuscript reviewers.

## REFERENCES

- Abatzoglou, J. T., & Williams, A. P. (2016). Impact of anthropogenic climate change on wildfire across western US forests. *Proceedings of the National Academy of Sciences*, 113(42), 11770–11775. doi:10.1073/pnas.1607171113
- Aguinis, H., Gottfredson, R. K., & Culpepper, S. A. (2013). Best-practice recommendations for estimating cross-level interaction effects using multilevel modeling. *Journal of Management*, 39(6), 1490–1528. doi:10.1177/0149206313478188
- Aksoy, H., & Wittenberg, H. (2011). Nonlinear baseflow recession analysis in watersheds with intermittent streamflow. *Hydrological Sciences Journal*, 56(2), 226–237. doi:10.1080/02626667.2011.553614
- Archfield, S. A., & Vogel, R. M. (2009). The implications of discretizing continuous random variables: An example using the U.S. Geological Survey reporting standards for streamflow data. In *Proceedings of the American Society of Civil Engineers World Environmental and Water Resources Congress* Kansas City, Missouri. doi: 10.1061/41036(342)519
- Baayen, R. H., Davidson, D. J., & Bates, D. M. (2008). Mixed-effects modeling with crossed random effects for subjects and items. *Journal of Memory and Language*, 59(4), 390–412. doi:10.1016/j.jml.2007.12.005
- Bart, R. R. (2016). A regional estimate of postfire streamflow change in California. *Water Resources Research*, 52(2), 1465–1478. doi:10.1002/2014WR016553
- Bart, R., & Hope, A. (2014). Inter-seasonal variability in baseflow recession rates: The role of aquifer antecedent storage in central California watersheds. *Journal of Hydrology*, 519, Part A, 205–213. doi:10.1016/j.jhydrol.2014.07.020
- Biswal, B., & Kumar, D. N. (2014). Study of dynamic behaviour of recession curves. *Hydrological Processes*, 28(3), 784–792. doi:10.1002/hyp.9604
- Biswal, B., & Marani, M. (2010). Geomorphological origin of recession curves. *Geophysical Research Letters*, 37(24), L24403. doi:10.1029/2010GL045415

- Blaney, H. F., & Criddle, W. D. (1962). Determining consumptive use and irrigation water requirements. Technical Bulletin 1275. US Department of Agriculture.
- Bogaart, P. W., van der Velde, Y., Lyon, S. W., & Dekker, S. C. (2016). Streamflow recession patterns can help unravel the role of climate and humans in landscape co-evolution. *Hydrology and Earth System Sciences*, 20(4), 1413–1432. doi:10.5194/hess-20-1413-2016
- Brutsaert, W., & Nieber, J. L. (1977). Regionalized drought flow hydrographs from a mature glaciated plateau. *Water Resources Research*, 13(3), 637–643.
- Callaway, R. M., & Davis, F. W. (1993). Vegetation dynamics, fire, and the physical environment in coastal Central California. *Ecology*, 74(5), 1567–1578. doi:10.2307/1940084
- Cannon, S. H., Gartner, J. E., Wilson, R. C., Bowers, J. C., & Laber, J. L. (2008). Storm rainfall conditions for floods and debris flows from recently burned areas in southwestern Colorado and southern California. *Geomorphology*, 96(3), 250–269. doi:10.1016/j.geomorph.2007.03.019
- Chapman, T. (1999). A comparison of algorithms for stream flow recession and baseflow separation. *Hydrological Processes*, 13(5), 701–714.
- Chen, X., & Wang, D. (2013). Evaluating the effect of partial contributing storage on the storage–discharge function from recession analysis. *Hydrology and Earth System Sciences*, 17(10), 4283–4296. doi:10.5194/hess-17-4283-2013
- Clark, M. P., Rupp, D. E., Woods, R. A., Tromp-van Meerveld, H. J., Peters, N. E., & Freer, J. E. (2009). Consistency between hydrological models and field observations: Linking processes at the hillslope scale to hydrological responses at the watershed scale. *Hydrological Processes*, 23(2), 311–319. doi:10.1002/hyp.7154
- Colman, E. A. (1951). Fire and water in southern California's mountains. California Forest and Range Experiment Station, US Department of Agriculture-Forest Service, Miscellaneous Paper #3.
- Cook, B. I., Ault, T. R., & Smerdon, J. E. (2015). Unprecedented 21st century drought risk in the American southwest and Central Plains. *Science Advances*, 1(1), e1400082. doi:10.1126/sciadv.1400082
- Crouse, R. P. (1961). First-year effects of land treatment on dry-season streamflow after a fire in southern California. Research Note #191. USDA Forest Service, Pacific Southwest Forest and Range Experiment Station, Berkeley, California.
- DeBano, L. F. (2000). The role of fire and soil heating on water repellency in wildland environments: A review. *Journal of Hydrology*, 231–232, 195–206. doi:10.1016/S0022-1694(00)00194-3
- Eidenshink, J., Schwind, B., Brewer, K., Zhu, Z.-L., Quayle, B., & Howard, S. (2007). A project for monitoring trends in burn severity. *Fire Ecology*, 3(1), 3–21. doi:10.4996/fireecology.0301003
- Enders, C. K., & Tofighi, D. (2007). Centering predictor variables in cross-sectional multilevel models: A new look at an old issue. *Psychological Methods*, 12(2), 121. doi:10.1037/1082-989X.12.2.121
- Falcone, J. A. (2011). GAGES-II: Geospatial attributes of gages for evaluating streamflow. US Geological Survey, Reston, VA. Retrieved from [http://water.usgs.gov/GIS/metadata/usgswrd/XML/gagesII\\_Sept2011.xml](http://water.usgs.gov/GIS/metadata/usgswrd/XML/gagesII_Sept2011.xml)
- Federer, C. A. (1973). Forest transpiration greatly speeds streamflow recession. *Water Resources Research*, 9(6), 1599–1604.
- Hadfield, J. D. (2010). MCMC methods for multi-response generalized linear mixed models: The MCMCglmm R package. *Journal of Statistical Software*, 33(2), 1–22.
- Hope, A., Tague, C., & Clark, R. (2007). Characterizing post-fire vegetation recovery of California chaparral using TM/ETM+ time-series data. *International Journal of Remote Sensing*, 28(6), 1339–1354. doi:10.1080/01431160600908924
- Hope, A., Decker, J., & Jankowski, P. (2008). Utility of gridded rainfall for IHACRES Daily River flow predictions in Southern California watersheds. *Journal of the American Water Resources Association (JAWRA)*, 44(2), 428–435. doi:10.1111/j.1752-1688.2008.00172.x
- Hope, A., Albers, N., & Bart, R. (2012). Characterizing post-fire recovery of fynbos vegetation in the Western Cape Region of South Africa using MODIS data. *International Journal of Remote Sensing*, 33(4), 979–999. doi:10.1080/01431161.2010.543184
- Hox, J. (2002). *Multilevel analysis: Techniques and applications*. Mahwah, NJ: Lawrence Erlbaum Associates.
- Ice, G. G., Neary, D. G., & Adams, P. W. (2004). Effects of wildfire on soils and watershed processes. *Journal of Forestry*, 102(6), 16–20.
- Imeson, A. C., Verstraten, J. M., van Mulligen, E. J., & Sevink, J. (1992). The effects of fire and water repellency on infiltration and runoff under Mediterranean type forest. *Catena*, 19(3–4), 345–361. doi:10.1016/0341-8162(92)90008-Y
- Ireland, G., & Petropoulos, G. P. (2015). Exploring the relationships between post-fire vegetation regeneration dynamics, topography and burn severity: A case study from the montane cordillera Ecozones of western Canada. *Applied Geography*, 56, 232–248. doi:10.1016/j.apgeog.2014.11.016
- Jencso, K. G., McGlynn, B. L., Gooseff, M. N., Wondzell, S. M., Bencala, K. E., & Marshall, L. A. (2009). Hydrologic connectivity between landscapes and streams: Transferring reach-and plot-scale understanding to the catchment scale. *Water Resources Research*, 45(4), W04428.
- Jung, H. Y., Hogue, T. S., Rademacher, L. K., & Meixner, T. (2009). Impact of wildfire on source water contributions in Devil Creek, CA: Evidence from end-member mixing analysis. *Hydrological Processes*, 23(2), 183–200. doi:10.1002/hyp.7132
- Keller, E. A., Valentine, D. W., & Gibbs, D. R. (1997). Hydrological response of small watersheds following the Southern California painted cave fire of June 1990. *Hydrological Processes*, 11(4), 401–414. doi:10.1002/(SICI)1099-1085(19970330)11:4<401::AID-HYP447>3.0.CO;2-P
- Kinoshita, A. M., & Hogue, T. S. (2011). Spatial and temporal controls on post-fire hydrologic recovery in Southern California watersheds. *Catena*, 87(2), 240–252. doi:10.1016/j.catena.2011.06.005
- Kinoshita, A. M., & Hogue, T. S. (2015). Increased dry season water yield in burned watersheds in Southern California. *Environmental Research Letters*, 10(1), 014003. doi:10.1088/1748-9326/10/1/014003
- Kirchner, J. W. (2009). Catchments as simple dynamical systems: Catchment characterization, rainfall-runoff modeling, and doing hydrology backward. *Water Resources Research*, 45(2), W02429. doi:10.1029/2008WR006912
- Le Maitre, D. C., Scott, D. F., & Colvin, C. (1999). Review of information on interactions between vegetation and groundwater. *Water SA*, 25(2), 137–152.
- Letey, J. (2001). Causes and consequences of fire-induced soil water repellency. *Hydrological Processes*, 15(15), 2867–2875. doi:10.1002/hyp.378
- Luce, C., Morgan, P., Dwire, K., Isaak, D., Holden, Z., & Rieman, B. (2012). *Climate change, forests, fire, water, and fish: Building resilient landscapes, streams, and managers*. US Department of Agriculture, Forest Service, Rocky Mountain Research Station: Fort Collins, CO.
- McMichael, C. E., & Hope, A. S. (2007). Predicting streamflow response to fire-induced landcover change: Implications of parameter uncertainty in the MIKE SHE model. *Journal of Environmental Management*, 84(3), 245–256. doi:10.1016/j.jenvman.2006.06.003
- McMichael, C. E., Hope, A. S., Roberts, D. A., & Anaya, M. R. (2004). Post-fire recovery of leaf area index in California chaparral: A remote sensing-chronosequence approach. *International Journal of Remote Sensing*, 25(21), 4743–4760. doi:10.1080/01431160410001726067
- Meixner, T., & Wohlgemuth, P. M. (2003). Climate variability, fire, vegetation recovery, and watershed hydrology. In *Proceedings of the First Interagency Conference on Research in the Watersheds* Benson, Arizona, pp. 651–656.
- Moore, R. D. (1997). Storage-outflow modelling of streamflow recessions, with application to a shallow-soil forested catchment. *Journal of Hydrology*, 198(1–4), 260–270. doi:10.1016/S0022-1694(96)03287-8
- Raudenbush, S. W., & Bryk, A. S. (2002). *Hierarchical linear models: Applications and data analysis methods*. Thousand Oaks, CA: Sage.

- Rupp, D. E., & Selker, J. S. (2006a). On the use of the Boussinesq equation for interpreting recession hydrographs from sloping aquifers. *Water Resources Research*, 42, W12421. doi:10.1029/2006WR005080
- Rupp, D. E., & Selker, J. S. (2006b). Information, artifacts, and noise in  $dQ/dt-Q$  recession analysis. *Advances in Water Resources*, 29(2), 154–160. doi:10.1016/j.advwatres.2005.03.019
- Shakesby, R. A., & Doerr, S. H. (2006). Wildfire as a hydrological and geomorphological agent. *Earth Science Reviews*, 74(3–4), 269–307. doi:10.1016/j.earscirev.2005.10.006
- Shaw, S. B., McHardy, T. M., & Riha, S. J. (2013). Evaluating the influence of watershed moisture storage on variations in baseflow recession rates during prolonged rain-free periods in medium-sized catchments in New York and Illinois, USA. *Water Resources Research*, 49, 6022–6028. doi:10.1002/wrcr.20507
- Silberstein, R. P., Dawes, W. R., Bastow, T. P., Byrne, J., & Smart, N. F. (2013). Evaluation of changes in post-fire recharge under native woodland using hydrological measurements, modelling and remote sensing. *Journal of Hydrology*, 489, 1–15. doi:10.1016/j.jhydrol.2013.01.037
- Spiegelhalter, D. J., Best, N. G., Carlin, B. P., & van der Linde, A. (2002). Bayesian measures of model complexity and fit. *Journal of the Royal Statistical Society, Series B (Statistical Methodology)* 64(4), 583–639. doi:10.2307/3088806
- Stegmueller, D. (2013). How many countries for multilevel modeling? A comparison of frequentist and Bayesian approaches. *American Journal of Political Science*, 57(3), 748–761. doi:10.1111/ajps.12001
- Szilagyi, J., Gribovszki, Z., & Kalicz, P. (2007). Estimation of catchment-scale evapotranspiration from baseflow recession data: Numerical model and practical application results. *Journal of Hydrology*, 336(1–2), 206–217. doi:10.1016/j.jhydrol.2007.01.004
- Tague, C., & Grant, G. E. (2009). Groundwater dynamics mediate low-flow response to global warming in snow-dominated alpine regions. *Water Resources Research*, 45, W07421. doi:10.1029/2008WR007179
- Tallaksen, L. M. (1995). A review of baseflow recession analysis. *Journal of Hydrology*, 165(1–4), 349–370. doi:10.1016/0022-1694(94)02540-R
- Tsang, Y.-P., Hornberger, G., Kaplan, L. A., Newbold, J. D., & Aufdenkampe, A. K. (2014). A variable source area for groundwater evapotranspiration: Impacts on modeling stream flow. *Hydrological Processes*, 28(4), 2439–2450. doi:10.1002/hyp.9811
- Tschinkel, H. M. (1963). Short-term fluctuation in streamflow as related to evaporation and transpiration. *Journal of Geophysical Research*, 68, 6459–6469.
- Watson, F., Vertessy, R., McMahon, T., Rhodes, B., & Watson, I. (2001). Improved methods to assess water yield changes from paired-catchment studies: Application to the Maroondah catchments. *Forest Ecology and Management*, 143(1–3), 189–204. doi:10.1016/S0378-1127(00)00517-X
- Wells, W. G. (1987). The effects of fire on the generation of debris flows in southern California. *Reviews in Engineering Geology*, 7, 105–114. doi:10.1130/REG7-p105
- Wittenberg, H. (1999). Baseflow recession and recharge as nonlinear storage processes. *Hydrological Processes*, 13(5), 715–726. doi:10.1002/(SICI)1099-1085(19990415)13:5<715::AID-HYP775>3.0.CO;2-N
- Wittenberg, H., & Sivapalan, M. (1999). Watershed groundwater balance estimation using streamflow recession analysis and baseflow separation. *Journal of Hydrology*, 219(1–2), 20–33. doi:10.1016/S0022-1694(99)00040-2
- Xiao, X., White, E. P., Hooten, M. B., & Durham, S. L. (2011). On the use of log-transformation vs. nonlinear regression for analyzing biological power laws. *Ecology*, 92(10), 1887–1894. doi:10.1890/11-0538.1
- Zecharias, Y. B., & Brutsaert, W. (1988). Recession characteristics of groundwater outflow and base flow from mountainous watersheds. *Water Resources Research*, 24(10), 1651–1658. doi:10.1029/WR024i010p01651

## SUPPORTING INFORMATION

Additional Supporting Information may be found online in the supporting information tab for this article.

**How to cite this article:** Bart RR, Tague CL. The impact of wildfire on baseflow recession rates in California. *Hydrological Processes*. 2017;31:1662–1673. <https://doi.org/10.1002/hyp.11141>